REPORT DOCUMENTATION PAGE

Form Approved
OMB No. 0704-0188

AD-A274 139

REPORT DATE	3. REPORT TYPE AND DATES COVERED
	Final Report 10Oct 92 - 30 Sep 93

4. TITLE AND SUBTITLE

Computer simulations of radiation generation from relativistic electron beams

5. FUNDING NUMBERS

AFOSR-91-0006

6. AUTHOR(S)

Dr Anthony T. Lin

7. PERFORMING ORGANIZATION NAME(S) AND ADDRESS(ES)

University of California
Department of Physics
Los Angeles CA 90024-1547

AFOSR-TR

8. PERFORMING ORGANIZATION REPORT NUMBER

93 0892

9. SPONSORING / MONITORING AGENCY NAME(S) AND ADDRESS(ES)

AFOSR/NE
110 Duncan Avenue
Bolling AFB DC 20332-0001

10. SPONSORING / MONITORING AGENCY REPORT NUMBER

2301/ES

11. SUPPLEMENTARY NOTES

12a. DISTRIBUTION / AVAILABILITY STATEMENT

UNLIMITED

This document has been approved for public release and sale; its distribution is unlimited.

12b. DISTRIBUTION CODE

13. ABSTRACT *(Maximum 200 words)*

This is the Final Technical Report on work performed under the support of the Air Force Office of Scientit Research under Grant AFOSR 91-0006 for the peridd October 1, 1992 to September 30, 1993. The objective of this work was to carry out basic physics research on the generation of coherent, tumable radiation from relativistic electron beams and exploring means of improving performance.

14. SUBJECT TERMS

15. NUMBER OF PAGES

16. PRICE CODE

17. SECURITY CLASSIFICATION OF REPORT	18. SECURITY CLASSIFICATION OF THIS PAGE	19. SECURITY CLASSIFICATION OF ABSTRACT	20. LIMITATION OF ABSTRACT
UNCLASSIFIED	UNCLASSIFIED	UNCLASSIFIED	UL

Computer Simulations of Radiation Generation From Relativistic Electron Beams

AFOSR 91-0006 Final Technical Report

Dr. Anthony T. Lin

UCLA Physics Department

University of California, Los Angeles

Department of Physics

Los Angeles, CA 90024-1547

COMPUTER SIMULATIONS OF RADIATION GENERATION FROM RELATIVISTIC ELECTRON BEAMS

AFOSR 91-0006

FINAL TECHNICAL REPORT

TO

AIR FORCE OFFICE OF SCIENTIFIC RESEARCH

Dr. Anthony T. Lin

Department of Physics

University of California, Los Angeles

Los Angeles, CA 90024-1547

October 1, 1992, to September 30, 1993

TABLE OF CONTENTS

I. Introduction

This is the Final Technical Report on work performed under the support of the Air Force Office of Scientific Research under Grant AFOSR 91-0006 for the period October 1, 1992 to September 30, 1993. The objective of this work was to carry out basic physics research on the generation of coherent, tunable radiation from relativistic electron beams and exploring means of improving performances.

II. Summary of Work Accomplished

This work covered computer simulations and theoretical studies of radiation generation in free electron microwave devices. We have carried out computer simulations and theoretical analyses to address various issues concerned with free electron devices which includes free electron lasers, gyro backward wave oscillators, and peniotron forward wave oscillators.

We have conceived a peniotron forward wave oscillator which relies on the pulse spreading of the forward propagating absolute instability in peniotron interaction to provide the feedback mechanism. Aside from the usual advantages (high efficiency at high harmonic operation) of peniotron interaction, the proposed scheme requires relatively short interaction length and can couple the wave power out from the beam exit side which render building a peniotron oscillator feasible and desirable.

We have devised a new concept for harmonic free electron lasers which is based on our early theoretical prediction that the axial guide field can be explored as a harmonic selection mechanism. Computer simulations were carried out which demonstrated that a second harmonic FEL based on the gyroresonance effect can attain gain and efficiency comparable to the fundamental FEL.

In order to interpretate the recent experimental results which show that gyro backward wave oscillators operated close to the waveguide cutoff can achieve much higher efficiency, computer simulations were performed. The results demonstrate that

one of the plausible mechanisms is the resulting initial large frequency mismatch (detuning) which places the electron bunch in an azimuthal phase close to where the maximum electron-wave coupling occurs.

To control the output phase of an oscillator, an external signal close to the free-running frequency is often injected to phase lock the oscillator. In carrying out computer simulations to illustrate the phase locking phenomenon, an unexpected effect that the injected signal also enhance the output efficiency is observed.

Below we summarize the scope and main findings of these investigations. More detailed information are contained in the appended reports.

A. Peniotron Forward Wave Oscillators (Appendix 1)

Microwave source based on peniotron mechanism was conceived almost three decades ago[1]. However, up to now there is still no convincing evidence to assure that high efficiency interaction has been achieved in any of the experiments reported. From the past experience a consensus has been reached that the essential elements for efficient peniotron operation are a vane waveguide and an axis-encircling beam.

An unavoidable feature of a vaned waveguide is the small frequency separation between the modes of larger azimuthal mode number n which renders the mode competition in peniotron device an important issue to be addressed. Using the parameters of Table I, the dispersion curves of the relevent waveguide modes are shown in Fig. 1. The first three cyclotron harmonic (s = 1, 2, 3) lines are also plotted in the same figure. There are three potential oscillation sources which are marked by points 1, 2 and 3. They all have their own starting oscillation lengths. Points 2 and 3 are the conventional gyrotron backward wave modes with relatively low efficiency. Point 1 is the peniotron mode.

In carrying out the stability analysis of a peniotron amplifier, we realized that the intrinsic feedback mechanism in an absolute instability even though is deleterious to an amplifier can be utilized to form oscillator without a cavity structure. An unstable system will, in general, be unstable for a range of k_z values and an initial disturbance will excite a spectrum of k_z's. In a weakly unstable system with beam current below the threshold of the absolute instability (point 1), the instability is convective. The disturbance propagates in the forward direction and the pulse will spread to each side of the peak. As the beam current is increased to such an extent so that the growth rate is strong enough to cause the signal to grow at the very point of the initial disturbance by pulse spreading, the instability becomes absolute. As is known that an absolute instability grows from the initial fluctuation of the system eigenmode and is eventually saturated by some nonlinear mechanism. Therefore by properly choosing the parameters one should be able to turn it into an useful microwave source. The time evolution of the wave power (TE_{31} mode) from the peniotron interaction at $z = 0$ and L ($L = 5$ cm) is plotted in Fig. 2a. The results clearly illustrate that initial perturbations grow in time at every point in the interaction space with the same growth rate which is the signature of an absolute instability. The direction of power flow determined by performing local Poynting flux calculation $\vec{E}_T \times \vec{B}_T$ is along the beam propagating direction and the output power attained more than 50% of the beam input power. The electron perpendicular velocity in the entire interaction space at $\omega_c t = 6000$ is displayed in Fig. 2b. Simulation results clearly reveal that as a result of the peniotron interaction all electrons irrespective of their initial phase give up their energies to the wave.

TABLE I

Second Harmonic Vaned Peniotron Oscillator Design

Beam Voltage	70 kV
Beam Current	3.5 A
Magnetic Field	6.5 kG
Mode	π mode
Number of Vanes	6
$\alpha = v_\perp / v_\parallel$	1.2
B_0 / B_g	1
$\omega_c / 2\pi$	33.65 GHz
Inner Circuit Radius (a)	0.16 cm
Outer Circuit Radius (b)	0.304 cm

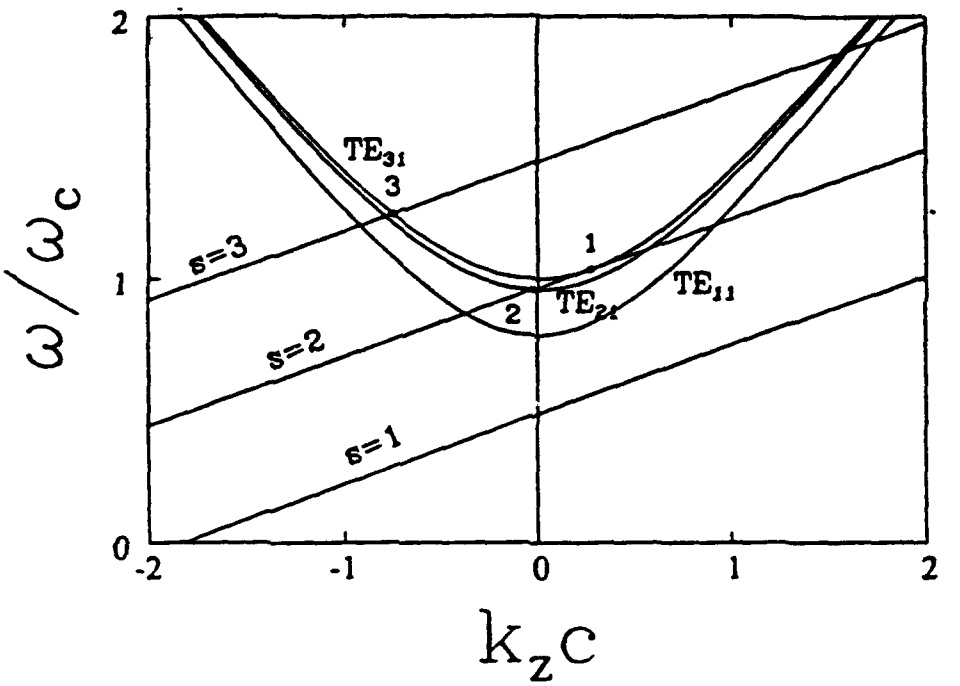

Figure 1: Dispersion cuves of a six vane slotted waveguide; potential self oscillation modes are marked by 1, 2 and 3.

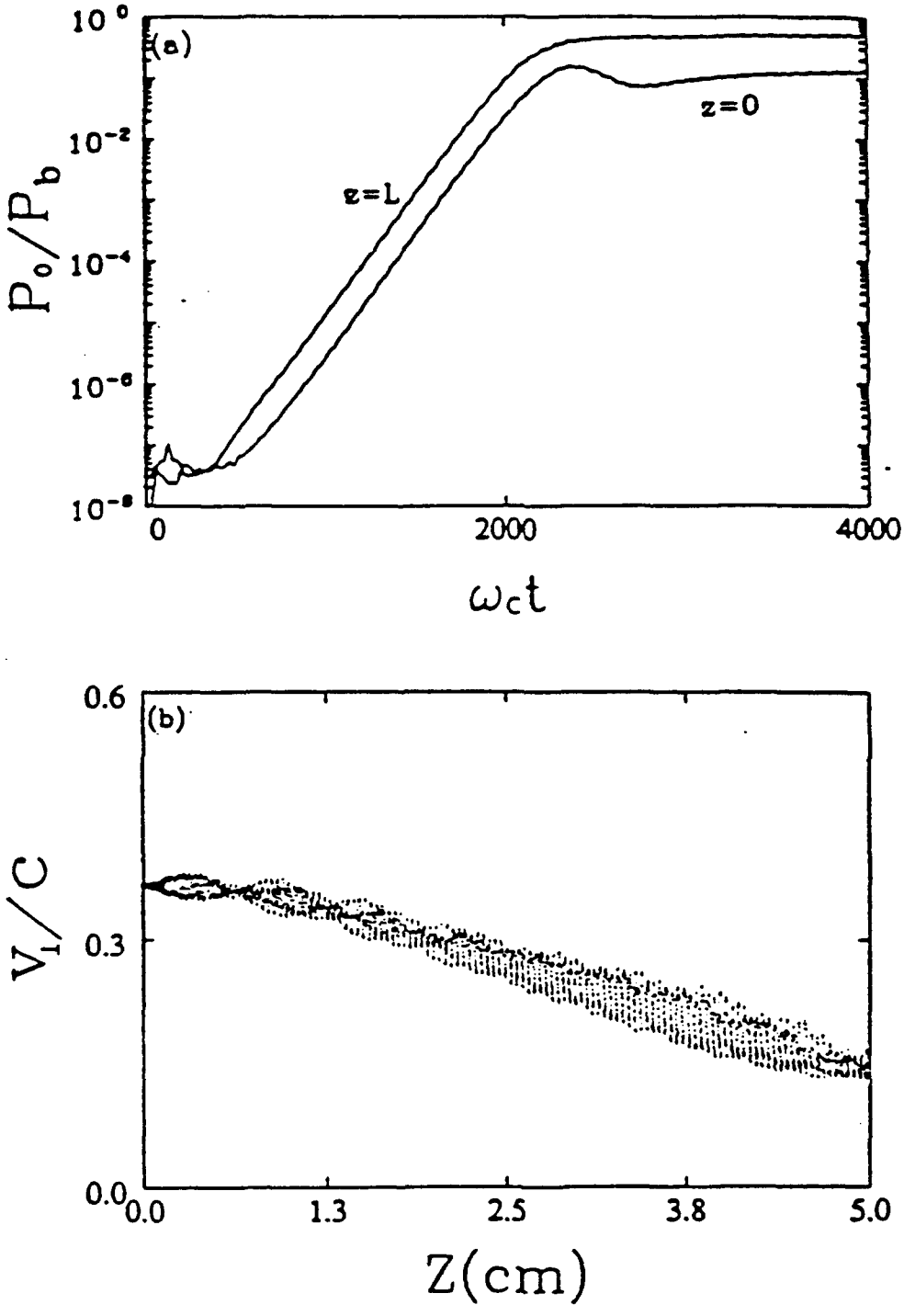

Figure 2: Self oscillation peniotron interaction with L = 5 cm: (a) time evolution of wave power (P_0) normalized to beam power (P_b) and (b) electron perpendicular velocity versus axial distance at $\omega_c t = 6000$.

B. A Harmonic FEL Based on The Second Harmonic Gyroresonance (Appendix 2)

In recent years, there is interest in the generation of harmonics in free electron lasers in an effort to achieve ever shorter wavelengths without the necessity of ever higher electron beam energies or shorter wiggler periods. The conventional approach for generating harmonic emission requires a strong wiggler field to produce a periodic longitudinal motion of electrons which produces gain in higher harmonics. In this scheme, a substantial part of beam kinetic energy is spent in exciting the fundamental emission and thus the harmonic radiation has often been limited by problems of insufficient gain and low efficiency. Therefore, harmonic FEL operation generally requires a mechanism that selectively enhances the competitiveness of a desired harmonic. We propose a different concept based on our early theoretical prediction[2] that the axial guide field can be explored as a harmonic selection mechanism. With the guide field tuned near to the nth wiggler harmonic, the *fundamental harmonic* component of the quiver velccity will be reduced by a factor approximately equal to n, whereas its nth-harmonic component is resonantly enhanced. The appropriate beam source for such an application is preferably annular in shape with a resonably large radius. So, upon resonant action in the wiggler region, the electrons will acquire a substantial harmonic quiver velocity with a minimum cross-sectional velocity spread. We have carried out computer simulations and demonstrated the feasibility of a second harmonic FEL based on the gyrosonance effect with attractive gain and efficiency. Preliminary results also indicate a susceptibility to interference from higher harmonic modes.

C. Dependence of Efficiency on Magnetic Field in Gyro Backward Wave Oscillators (Appendix 3)

One of the advantages of utilizing gyro BWO as millimeter wave source is its tunability through varying the magnetic field. Therefore it is important to investigate how the variation of magnetic field influences the output efficiency. As is expected simulation results show that the output frequency scales almost linearly with the magnetic field in most of the region except very near the cutoff while the output efficiency exhibits a significant jump (about 50%) when the oscillation frequency approaches the waveguide cutoff frequency. As a result a roughly constant output power gyro BWO can be operated in the following two regimes: high efficiency with about 8% tunability or medium efficiency with about 40% tunability.

In the case of $\omega_0 = 1.043\ \omega_c$ the output effieciency is about 20%. This is in good agreement with the result of a recent experiment[3]. In order to illustrate how the electron azimuthal bunching process differs when the magnetic field is varied, the phase trajectories of forty test electrons initially ($z = 0$) uniformly distributed between 0 and 2π are followed. Simulation results show that one of the plausible mechanisms for this high efficiency operation is the resulting substantially larger frequency mismatch (detuning) which places the electron bunch close to $\theta = \frac{\pi}{2}$ where the maximum electron-wave coupling takes place. At the same time the group velocity of the wave in this case is also slower which increases the electron-wave interaction time. These have all contributed to the enhancement of output efficiency.

D. Phase Locking of Gyro Backward Wave Oscillators

Injecting a weak signal into a more powerful free-running gyrotron backward wave oscillator can produce interesting and useful effects, such as controlling the phase of the output wave. A series of simulations have been carried out to study the phase locking phenomenon by using the configuration of the recent experimental set-up[3]. The scheme for diagnosing whether an oscillator has been phase locked or not is

by mixing the injected signal (ω_i) with the output signal (ω_o) and taking the time averaging over one injected signal period.

$$\phi(t) = \tan^{-1}\left\{ \frac{< E_0(t)\ \sin\omega_i t >}{< E_0(t)\ \cos\omega_i t >} \right\}$$

$$= \Delta\omega_0 t - \phi_i \quad , \qquad (1)$$

where $\Delta\omega_0 = \omega_i - \omega_0$ and ϕ_i is the phase difference. The ouutput wave is phase locked by the input signal if $\phi(t)$ asymtotically approaches a constant. Figure 3 shows the simulation results using $\Delta\omega_0 = 1 \times 10^{-3}\ \omega_0$ and $P_i/P_0 = -15$dB. The external signal was injected after the output power reached steady-state ($\omega_c t = 4000$). Figure 3b clearly illustrates that $\phi(t)$ asymptotically approaches a constant which is the signature of phase locking. The conventional theory predicts that the output power can only be increased by the amount of the injected signal power. Figure 3a reveals that in the presence of the injected signal the output power is enhanced by almost 50%. This unexpected effect requires more study. In contrast to the classical oscillator, the quality factor of a gyro backward wave oscillator is undefined which could complicate the theoretical analysis.

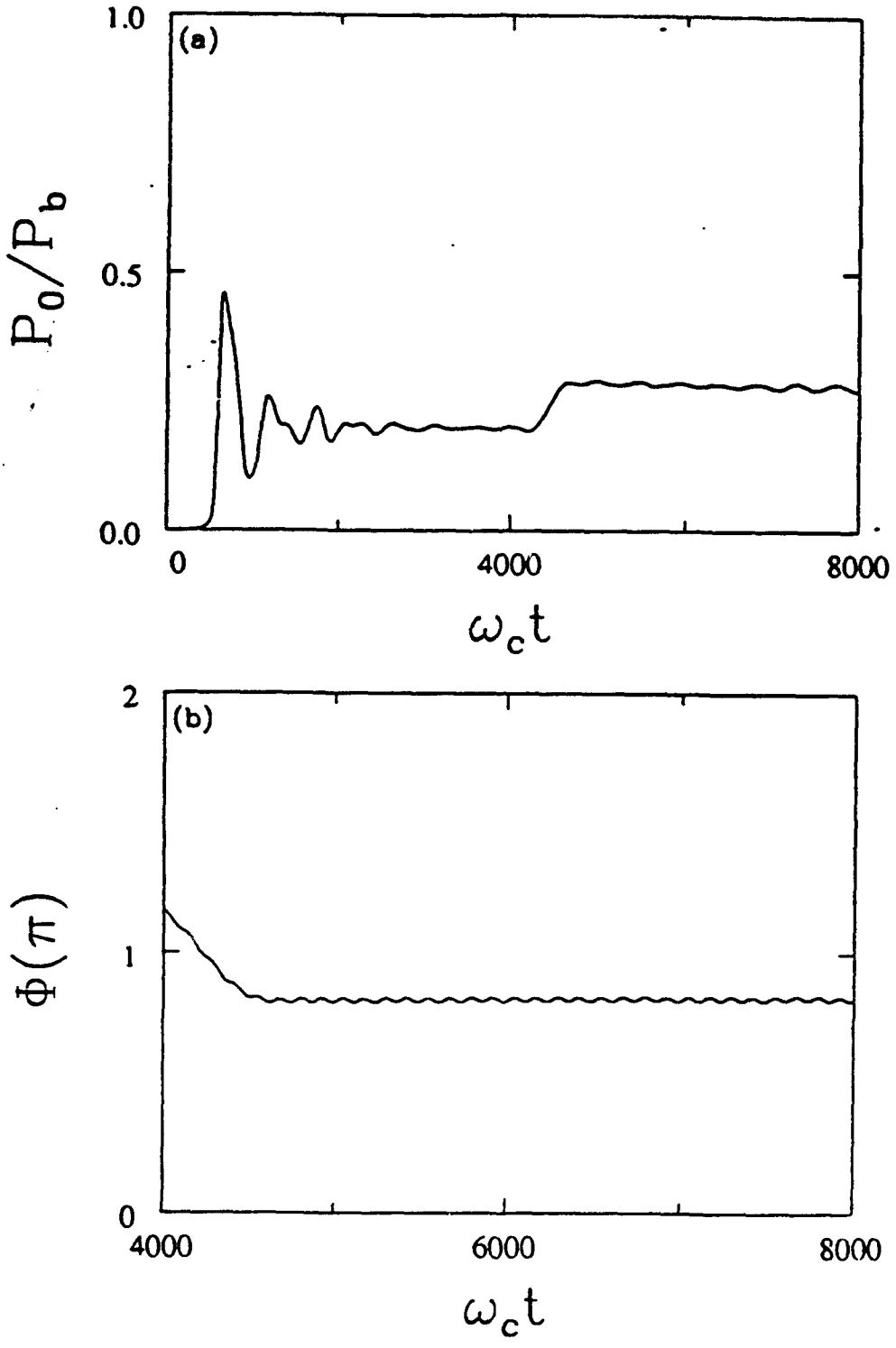

Figure 3: Gyro backward wave oscillator with an external signal:

(a) output pulse and (b) showing injection locking.

III. AFOSR Supported Publications (October 1, 1992--September 30, 1993)

1. A.T. Lin, "Mechanisms of Efficiency Enhancement in Tapered Gyro Backward Wave Oscillators," Physics Review A. 46, R4516(1992).
2. Q.S. Wang, D.B. McDermott, C.S. Kou, A.T. Lin, K.R. Chu, N.C. Luhmann, and J. Pretterebner, "High-Power Second Harmonic Gyro-TWT Amplifier," Digest of Int. Electron Device Meeting, 394(1992).
3. A.T. Lin and Chih-Chien Lin, "Dependence of Efficiency on Magnetic Field in Gyro Backward Wave Oscillators," accepted for publication in Physics of Fluids B, (1993).
4. A.T. Lin and K.R. Chu, "A Harmonic FEL Based on The Second Harmonic Gyroresonance," accepted for publication in Nuclear Instruments And Methods in Physics Research (1993).
5. A.T. Lin and Chih-Chien Lin, "Peniotron Oscillators Without Cavity Structures," submitted to Physical Review Letters (1993).

APPENDICES

1. Peniotron Forward Wave Oscillators.

2. A Harmonic FEL Based on the Second Harmonic Gyroresonance.

3. Dependence of Efficiency on Magnetic Field In Gyro Backward Oscillators.

APPENDIX 1

Gyro Peniotron Forward Wave Oscillators

A.T. Lin and Chih-Chien Lin

Department of Physics

University of California at Los Angeles

Los Angeles, CA 90024-1547

Aug. 1993

Abstract

The pulse spreading of the forward propagating absolute instability in gyro-peniotron interaction can be utilized to provide the feedback mechanism for establishing forward wave oscillators. By properly choosing the interaction length and beam current high efficiency stable output at high harmonic operation can be attained. This is demonstrated by performing computer simulations which also reveal that the peniotron interaction is able to suppress the gyrotron interaction and reaches the optimal efficiency without the influence of the gyrotron mode.

I. Introduction

Microwave source derived from peniotron mechanism was conceived almost three decades ago[1]. Since then many investigators have carried out theoretical calculations[2-5] and attempted to employ various beam and electrodynamic configurations[6,7] to illustrate the aspect of high efficiency peniotron harmonic interaction. Up to now there is still no convincing evidence to assure that high efficiency interaction has been achieved in any of the experiments. However from the past experience a consensus has been reached that the essential elements for efficient peniotron operation are a electrodynamic configuration which is capable of providing a positive radial gradient in the microwave field distribution and an axis-encircling beam which initially can be placed at a high beam-wave coupling position. Recently, based on these important informations, the parameters of a peniotron amplifier[8] were proposed and a high quality factor ($Q \simeq 2000$) peniotron oscillator was built[7]. The former has to avoid various self oscillations which could degrade or totally prohibit the amplification process. This constraint forces one to contemplate a multi-section device with the length of each section below the starting oscillation length of all the potential oscillations. The high quality factor of the latter tends to require a well matched external load to couple out the major portion of the stored energy. It is also suspected that the experimental peniotron output[7] may be contaminated by the nearby gyrotron oscillation. In this paper we propose an alternative peniotron oscillator configuration without external reflection which alleviates the difficulty of finding a well matched load circuit. The feedback mechanism is provided by the pulse spreading of the forward propagating absolute instability which can be chosen to be the dominant interaction in the system. The proposed configuration may be considered as the first step to demonstrate that peniotron interaction is capable of attaining high efficiency. In investigating the peniotron and gyrotron competition, simulation results reveal that the

peniotron interaction always suppresses the gyrotron interaction if the beam guiding center spread is moderate (< 30 %). This understanding should be helpful in interpretating the experimental result of conventional peniotron oscillators[7]. Simulation results are also capable of determining the starting oscillation length of absolute instability which is an important information for a peniotron amplifier.

II. Numerical Model

Because of its boundary conditions, the harmonic field in an azimuthally corrugated interaction structure originally introduced for high harmonic gyrotron operations[9,10] becomes stronger when it gets closer to the waveguide wall and is therefore also suitable for the peniotron interaction. The cross-sectional view of a six vane slotted waveguide with an axis-encircling beam is displayed in Fig. 1a. In the interaction region, the electric and magnetic fields of a transverse electric field mode[11,12] may be written as

$$E_n = E_{Tn}(z,t)\,(\hat{z} \times \nabla_\perp C_n) \tag{1}$$

$$B_n = B_{Tn}(z,t)\,\nabla_\perp C_n + \hat{z}\,B_{Ln} k_\perp C_n \tag{2}$$

where C_n is the local wave function

$$C_n = -\sum_{m=-\infty}^{\infty} \frac{A_\Gamma}{k_\perp} J_\Gamma(k_\perp r)\, e^{i\Gamma\theta} \quad . \tag{3}$$

Here $\Gamma = n + mN$, $n = 0,1,\ldots., N/2$, m is any integer, N is the number of vanes, and

$A_\Gamma = \frac{N\theta_0}{\pi} \cdot \frac{\sin\Gamma\theta_0}{\Gamma\theta_0}$ is the enhancement factor of the slotted structure. $k_\perp$ is the cutoff wavenumber which can be determined from the circuit dispersion relation

$$\sum_\Gamma \frac{J_\Gamma(k_\perp a)}{J_\Gamma'(k_\perp a)} \left(\frac{\sin\Gamma\theta_0}{\Gamma\theta_0} \right)^2 = -\frac{\pi}{N\theta_0} \frac{Z_0(k_\perp a)}{Z_1(k_\perp a)} , \qquad (4)$$

where Z_Γ is a combination of Bessel function (J_Γ) and Neumann function (N_Γ) of order Γ

$$Z_\Gamma(x) = J_\Gamma(x) - \frac{J_1(k_\perp b)}{N_1(k_\perp b)} N_\Gamma(x) , \qquad (5)$$

and $\theta_0 = 2\pi / 4N$. Here a and b denote respectively the inner and outer circuit radius. For each value of n, there are infinite number of solutions from Eq.(4). The first root is the most important one and the associated mode is usually designated by TE_{n1}. The mode number n is also the number of times the RF field pattern repeats in one rotation around the waveguide axis. There are many possible modes but the two most interesting cases are the π mode where adjacent slots are out of phase by π, and the 2π mode where the phase in each slot is identical. In the most rigorous description an infinite superposition of different Γ's is required to represent each n mode. However in most of the cases an adequate approximation includes just two partical waves - those with $\Gamma = n$ and $(n - N)$. The physical meaning of this is that an electromagnetic wave rotating in a periodic structure must interfer with other waves to reproduce the static periodic pattern of the structure.

The modes supported by the slotted structure can interact with an axis-encircling electron beam through the relativistic gyrotron and non-relativistic peniotron

mechanisms. In a gyrotron interaction it is necessary that an electron stays approximately in the same phase with respect to the wave as it traverses through the interaction region so that the cumulative electron-wave interaction produces a substantial bunching through relativistic mass effect. As a consequence, an initially randomly phased electron beam would end up with some of its electrons giving up energy to and the rest of them absorbing energy from the same wave. This resonant condition can be expressed as

$$\omega_0 = k_z v_z + s\frac{\Omega_c}{\gamma} \quad , \tag{6}$$

where ω_0 and k_z are respectively the wave frequency and axial wavenumber. v_z and γ are the electron axial velocity and relativistic factor. Ω_c is the non-relativistic cyclotron frequency and s is the harmonic number. For efficient gyrotron interaction n must be equal to s. On the other hand the gain mechanism underlines a peniotron interaction is due to the electron guiding center drift so that during a cyclotron orbit an electron on the average is in a stronger RF field region during the decelerating phase and in a weaker RF field region during the accelerating phase. This is due to the fact that an accelerated electron increases its radius of gyration and the requirement $n = s + 1$ which ensures that in our example (Fig. 1a) half of the cyclotron orbit is accelerating while the other half is decelerating. As a result all electrons regardless of their initial phases relative to the wave convert their kinetic energy into wave energy and makes peniotron devices inherently high-efficiency.

An unavoidable feature of a vaned waveguide is the small frequency separation between the modes of larger n which renders the mode competition in peniotron device an important issue to be addressed. Using the parameters of Table I, the

dispersion curves of the relevent waveguide modes are shown in Fig. 1b. The first three cyclotron harmonic (s = 1, 2, 3) lines are also plotted in the same figure. There are three potential oscillation sources which are marked by points 1, 2 and 3. They all have their own starting oscillation lengths. Points 2 and 3 are the conventional gyrotron backward wave modes with relatively low efficiency. Point 1 is the desired peniotron mode which is capable of producing high efficiency output as well as large temporal growth rate due to its grazing interaction.

III. Simulation Results

The intrinsic feedback mechanism in an absolute instability even though is deleterious to an amplifier can be utilized to form an oscillator without a cavity structure. Gyrotron backward wave oscillators[13,14] which rely on a backward propagating electromagnetic wave to feedback the energy generated by the forward propagating beam have been built and performed rather well. As far as the absolute unstable mode at point 1 (Fig. 1b) is concerned, experiments carried out so far were designed to avoid the excitation of this mode by using parameters below its starting oscillation condition.

The theoretical investigations of the absolute instability for either gyrotrons[15,16] or peniotrons[17] are all based on the pinch-point theory which was first derived in plasma physics for an infinite homogeneous medium[18]. However, an absolute instability in a limited spatial extent may be stable. In order to illustrate the effects of system length on the competition among various absolute unstable modes, we have first carried out single transverse mode computer simulations to evalute their temporal growth rate versus interaction length and results are shown in Fig. 2a. The starting oscillation length can be determined by extending the growth rate curve to intersect the z axis. The time evolution of the wave power (TE_{31} mode) from the peniotron

interaction at z = 0 and L for the L = 5 cm case is plotted in Fig. 2b. The results clearly illustrate that initial perturbations grow in time at every point in the interaction space with the same growth rate which is the signature of an absolute instability. The direction of power flow determined by performing local Poynting flux calculation $\vec{E_T} \times \vec{B_T}$ is along the beam propagating direction and the output power attained more than 50% of the beam input power. It was also observed in simulations that a broad spectrum of k's was excited and they all propagate in the forward direction. In the range of $L \leq 10$ cm, there is no trace of exciting the backward wave of point 3 (Fig. 1b). Using the same system length and retaining only the TE_{21} mode, the time evolution of the wave power at both ends is shown in Fig. 2c. In this case the instability arises from the gyrotron backward wave interaction. The efficiency has reached only about 10% and the wave power flow is in the backward direction. Notice that the wave amplitude at z = L is not negligible in comparison with that of at z = 0 because point 2 (Fig. 1b) is so close to the waveguide cutoff. In order to demonstrate the difference between the peniotron and the gyrotron interactions, their respective electron perpendicular velocity in the entire interaction space at $\omega_c t \approx 6000$ is displayed in Fig. 3. Simulation results clearly reveal that as a result of the peniotron interaction all electrons irrespective of their initial phase give up their energies to the wave while the gyrotron interaction results in that only part of electron beam loses energy and the remaining part gains energy.

An unstable system will, in general, have a range of k_z values with positive $\omega_i(k_z)$ and an initial disturbance will excite a spectrum of k_z's. In a weakly unstable system with beam current below the threshold for oscillation, the instability is convective. The disturbance like point 1 in Fig. 1b propagates in the forward direction and the pulse will spread to each side of the peak. As the beam current is increased to such an extent so that the growth rate is strong enough to cause the signal to grow at

the very point of the initial disturbance by pulse spreading, the instability becomes absolute.

The threshold of the absolute instability in an infinite system can be evaluated by using the expression derived in Ref. [19] which describes the spatial and temporal evolution of the response electric field to a localized initial disturbance

$$E(z,t) = \frac{1}{[2\pi i\omega''(k_0)t]^{1/2}} \exp\left[ik_0z - i\omega(k_0)t + \frac{i(z-v_gt)^2}{2\omega''(k_0)t}\right], \qquad (7)$$

where $\omega=\omega(k)$ is the dispersion relation for the peniotron interaction[14], $v_g = \omega_r'(k_0)$ where k_0 is such that $\omega_i'(k_0) = 0$ and $\omega_i''(k_0) < 0$ and the prime is the derivative with respect to k_z. Equation (7) reveals that the evolving pulse peaks at $z=v_gt$, the pulse shape is growing and spreading in time if $\omega_i''(k_0)$ is negative, and its mean-square spatial spread is the reciprocal of $Im[\frac{1}{\omega''(k_0)t}]$. The threshold can be determined from the fact that $E(z=0,t)$ must increase exponentially with time or

$$Im[\omega(k_0)] > Im\left[\frac{v_g^2}{2\omega''(k_0)}\right], \qquad (8)$$

This expression only gives an approximate threshold for self oscillation in an infinite system. By substituting the parameters used in simulations into the dispersion relation given in Ref. [17], we obtained respectively 0.0157 ω_c for the left hand side and 0.014 ω_c for the right hand side of Eq. (8). Clearly, the inequality in Eq. (8) is satisfied. The evidence of spatial pulse spreading at early time can also be infered indirectly from Fig. 4a which displays the time evolution of unstable pulse in wave number space before the stored energy begins to exponentiate in time. Notice that the pulse width in

real and k_z space is inversely proportional to each other. The width of the unstable k_z spectrum remains relatively constant during the wave growing period (Fig. 4b). As is known that an absolute instability grows from the initial fluctuation of the system eigenmodes and is eventually saturated by some nonlinear mechanism. Therefore by properly choosing the parameters one should be able to turn it into an useful microwave source. Based on our prelimary simulation results which will be presented later, the proposed mechanism possesses certain unique characteristics which make it a very attractive and viable peniotron microwave source.

To assure that the oscillation from the TE_{21} mode would not deteriorate the performance of the desired peniotron operation, multimode simulations were carried out. Figure 5 shows the time evolution of the stored energy in the interaction space for three different cases. With L = 5 cm (Fig. 5a) the initial growth of the TE_{21} mode comes from the convective unstable mode with positive k_z and the growth rate of its absolute unstable mode is so small that it can be easily suppressed by the growth of the TE_{31} mode. Lengthening the system length to 8 cm tends to enhance the gyrotron interaction more than to the peniotron interaction. In this case the two interactions have about the same growth rate (Fig. 5b). The peniotron mode eventually is able to suppress the gyrotron mode. Using L = 8 cm and I = 1.5 A (Fig. 5c) the temporal growth rate of the gyrotron interaction now surpasses that of the peniotron interaction. However the peniotron interaction is still able to suppress the gyrotron interaction. The respective time evolution of the peniotron output power of the three cases described in Fig. 5 is shown in Fig. 6. Both single mode and two modes simulations are presented. The results indicate that the presence of the gyrotron interaction when it reaches large amplitude may affect the temporal growth rate of the peniotron interaction which requires no phase bunching but not its final efficiency for all three cases. This is because that to a peniotron interaction a saturated gyrotron mode induces effective

beam guiding center and perpendicular velocity spreads which would reduce the temporal growth rate. Since at the end the gyrotron mode is completely suppressed and returns to its noise level, the peniotron mode should be able to attain the efficiency without the influence of the gyrotron mode. The effects of guiding center spread and beam current on the performance of the oscillator (L=5 cm) are respectively displayed in Fig. 7a and Fig. 7b. The results show that a 20% guiding center spread would degrade the output efficiency to 40% and I = 3.5 A is the optimal beam current for maximizing the effieciency. The optimal system length (L_0) which maximizes the output efficiency is very close to 5 cm (I = 3.5 A). With $L > L_0$, most of the electrons (in the $z > L_0$ region) due to changes in their energy and guiding center location resulting from electron-wave interactions are no longer axis encircling and eventually becomes resonance with the wave. As a result of detuning, electrons on the average start to absorb energy from the wave and terminates the wave growth process.

IV. Summary

In summary, we have proposed a scheme for establishing peniotron forward wave oscillator without external reflection. The feedback mechanism relies on the pulse spreading of the absolute instability. Simulation results also reveal that the peniotron interaction is capable of suppresing the gyrotron interaction. This suppression phenomenon should also occur in a conventional peniotron oscillator which requires less beam current to start the interaction.

ACKNOWLEDGEMENT

This work was supported by the Air Force Office Of Scientific Research under Grant No. AFOSR 91-0006 and the San Diego Supercomputing Center.

REFERENCES

1. K. Yamanouchi, S. Ono, and Y. Shibata, Proc. 5th International Microwave Tube Conference, Paris, 321(1964).
2. S. Ono, K. Tsutaki, and T. Kageynama, Int. J. Electron, 56, 507(1984).
3. P. Vitello, Int. J. of Infrared and Millimeter Waves, 8, 487(1987).
4. A.K. Ganguly, S. Ahn, and S.Y. Park, Int. J. Electron, 65, 597(1988).
5. P.S. Rha, L.R. Barnett, J.M. Baird, and R.W. Grow, IEEE Trans. on Electron Devices, 36, 789(1989).
6. G. Döhler, D. Gallagher, C. Lowrie, R. Moats, and F. Scafuri, Int. Electron Device Meeting, 845(1984).
7. K. Yokoo, H. Shimawaki, H. Tadano, T. Ishihara, K. Sagae, N. Sato, and S. Ono, 17th Int. Conf. on Infrared and Millimeter Waves, 498(1992).
8. G.S. Park, J.L. Hirshfield, R.H. Kyser, C.M. Armstrong, and A.K. Gauguly, 17th Int. Conf. on Infrared and Millimeter Waves, 500(1992).
9. Y.Y. Lau and L.R. Barnett, Int. J. Infrared and Millimeter Waves, 3, 619(1982).
10. K.R. Chu and D. Dialetis, Infrared and Millimeter Waves, 13, Academic Press, New York, 45(1985).
11. N.M. Kroll and E.L. Willis, J. Appl. Phys, 19, 166(1947).
12. T.H. Kho and A.T. Lin, Nuclear Instruments and Methods in Phys. Research, A296, 642(1990).
13. T.A. Spencer, R.M. Gilgenbach, J.J. Choi, J. Appl. Phys. 72, 1221(1992).
14. C.S. Kou, S.H. Chen, L.R. Barnett, H.Y. Chen and K.R. Chu, Phys. Rev. Letts. 70, 924(1993).
15. K.R. Chu and A.T. Lin, IEEE Trans.-Plasma Science, 16, 90 (1988).
16. J.A. Davis, Phys. Fluids, B1, 663(1989).
17. A.K. Ganguly, Y.Y. Lau, and S. Ahn, Phys. Fluids B4, 3800(1992).
18. A. Bers, A.K. Ram, and G. Francis, Phys. Rev. Lett. 53,1457(1984).
19. T. Stix, Waves in Plasma, Chapter 9, American Institute of Physics (1992).

TABLE I

Second Harmonic Vaned Peniotron Oscillator Design

Beam Voltage	70 kV
Beam Current	3.5 A
Magnetic Field	6.5 kG
Mode	π mode
Number of Vanes	6
$\alpha = v_\perp / v_\parallel$	1.2
B_0 / B_g	1
$\omega_c / 2\pi$	33.65 GHz
Inner Circuit Radius (a)	0.16 cm
Outer Circuit Radius (b)	0.304 cm

Figure Captions:

Figure 1 Six vane slotted waveguide and an axis encircling beam: (a) cross-sectional view and (b) dispersion curves.

Figure 2 Self oscillations in finite length system: (a) temporal growth rate versus system length (star: TE_{31}, circle: TE_{21}) and the time evolution of wave power(P_0) normalized to beam power (P_b) for L = 5 cm (b) peniotron interaction (TE_{31}) and (c) gyrotron interaction (TE_{21}).

Figure 3 Electron perpendicular velocity versus axial distance: (a) peniotron interaction and (b) gyrotron interaction.

Figure 4 Time evolution of the unstable k_z spectrum: (a) before the stored energy begins to grow and (b) during the growth.

Figure 5 Time evolution of stored wave energy from multi mode simulations. (a) L = 5 cm, I =3.5 A, (b) L = 8 cm, I = 3.5 A, and (c) L = 8 cm, I = 1.5 A.

Figure 6 Time evolution of peniotron output wave power (solid curve is from single mode simulation, dashed curve is from multi mode simulation : (a) L = 5 cm, I =3.5 A, (b) L = 8 cm, I = 3.5 A, and (c) L = 8 cm, I = 1.5 A.

Figure 7 Effects of (a) guiding center spread and (b) beam current on the performance of the oscillator.

(a)

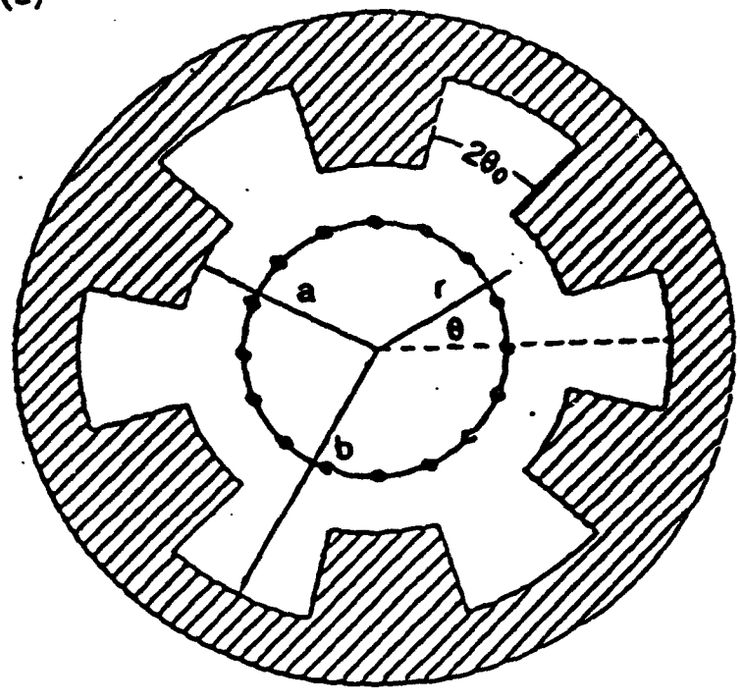
$2\theta_0$
a
r
θ
b

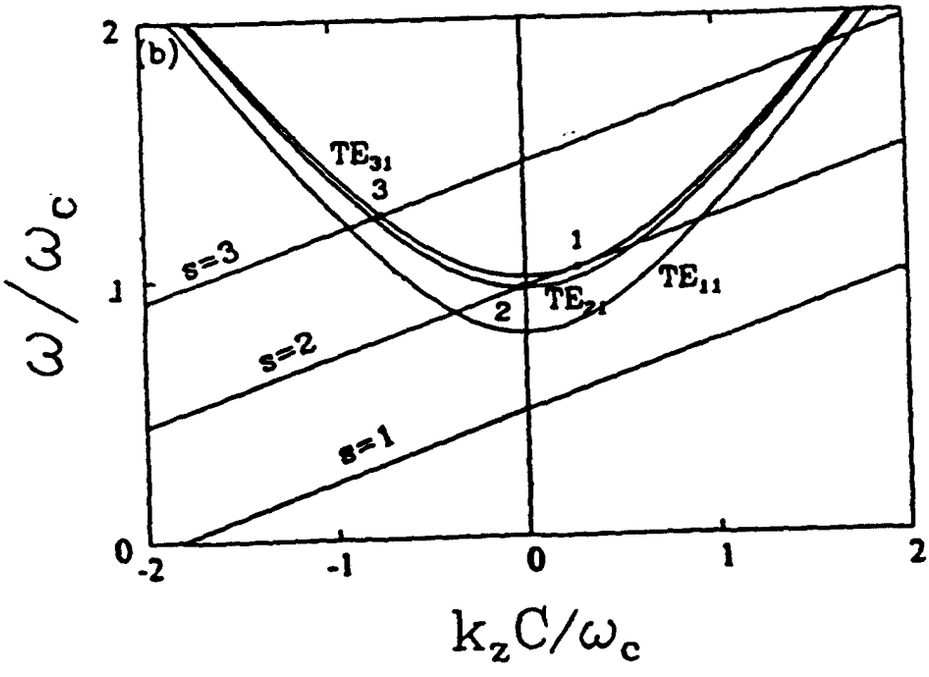
(b)
2
1
0
-2
-1
0
1
2
ω/ω_c
$k_z C/\omega_c$
TE_{31}
3
1
TE_{21}
2
TE_{11}
s=3
s=2
s=1

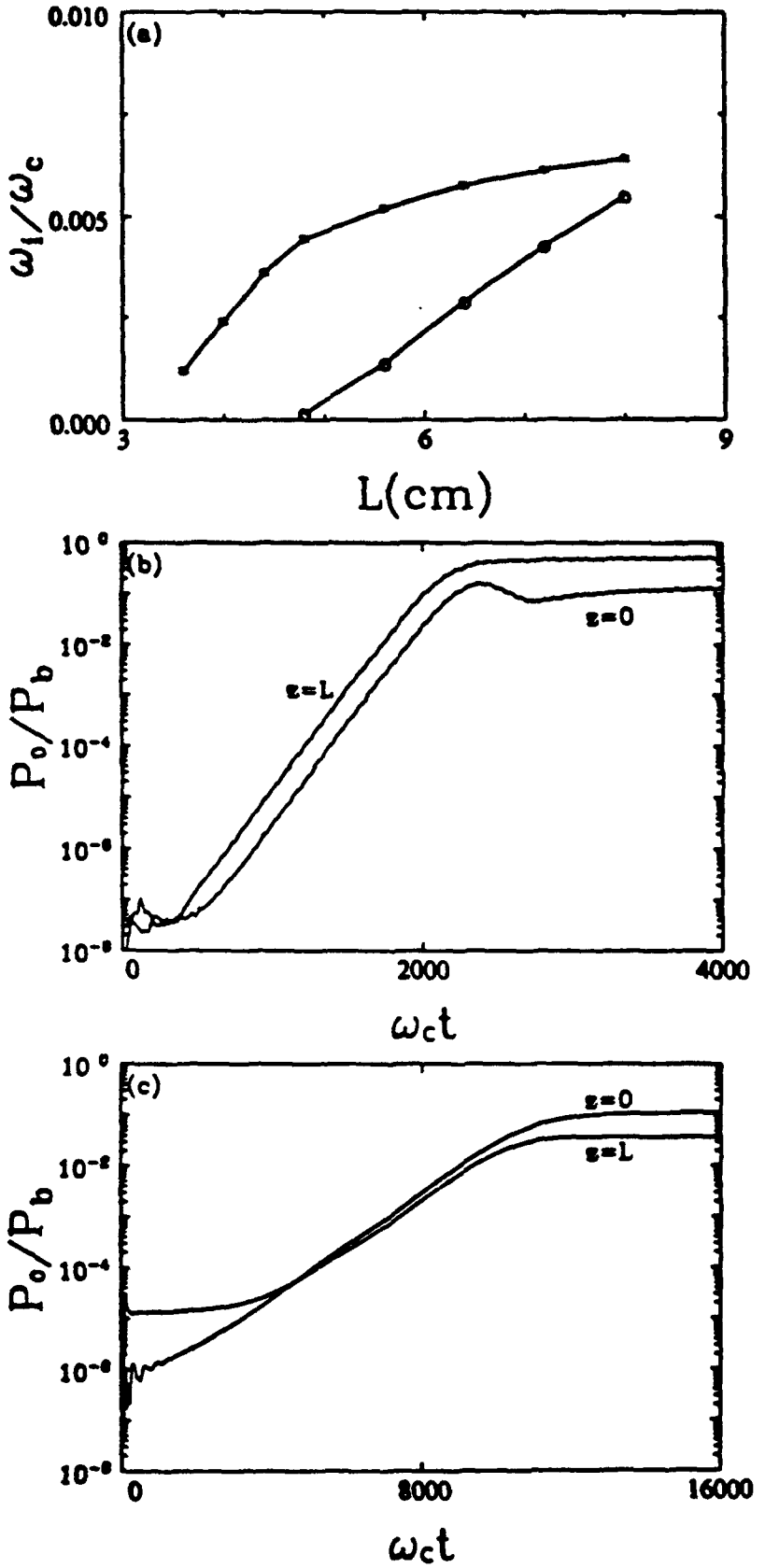
(a)
0.010
0.005
0.000
ω_l/ω_c
3
6
9
L(cm)
(b)
10^0
10^{-2}
10^{-4}
10^{-6}
10^{-8}
P_o/P_b
z=L
z=0
0
2000
4000
$\omega_c t$
(c)
10^0
10^{-2}
10^{-4}
10^{-6}
10^{-8}
P_o/P_b
z=0
z=L
0
8000
16000
$\omega_c t$

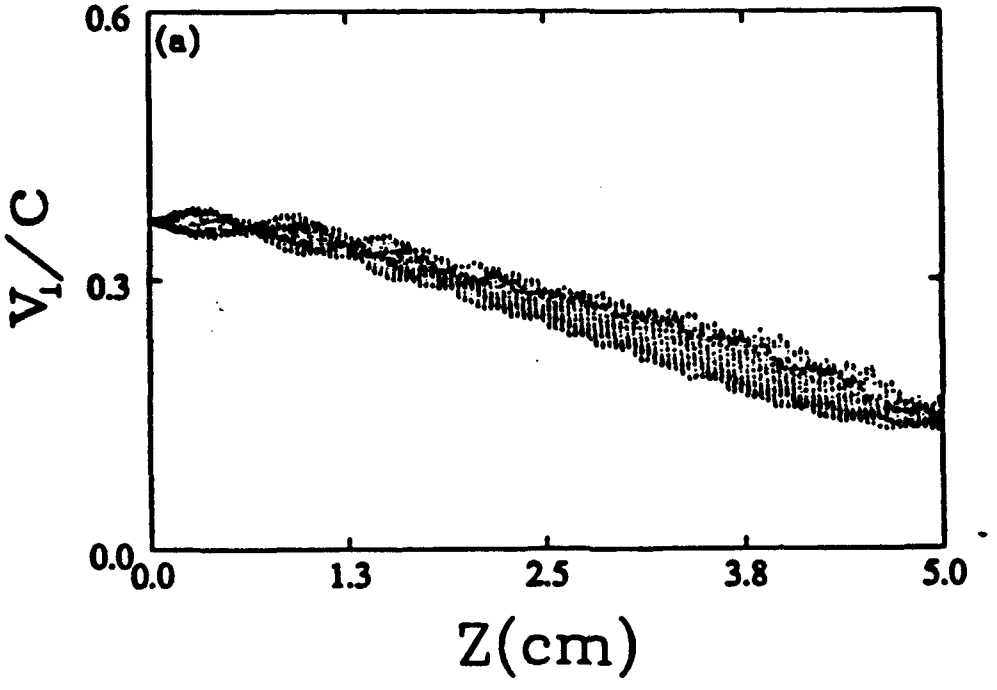
(a)
0.6
0.3
0.0
$V_\perp/C$
0.0
1.3
2.5
3.8
5.0
Z(cm)

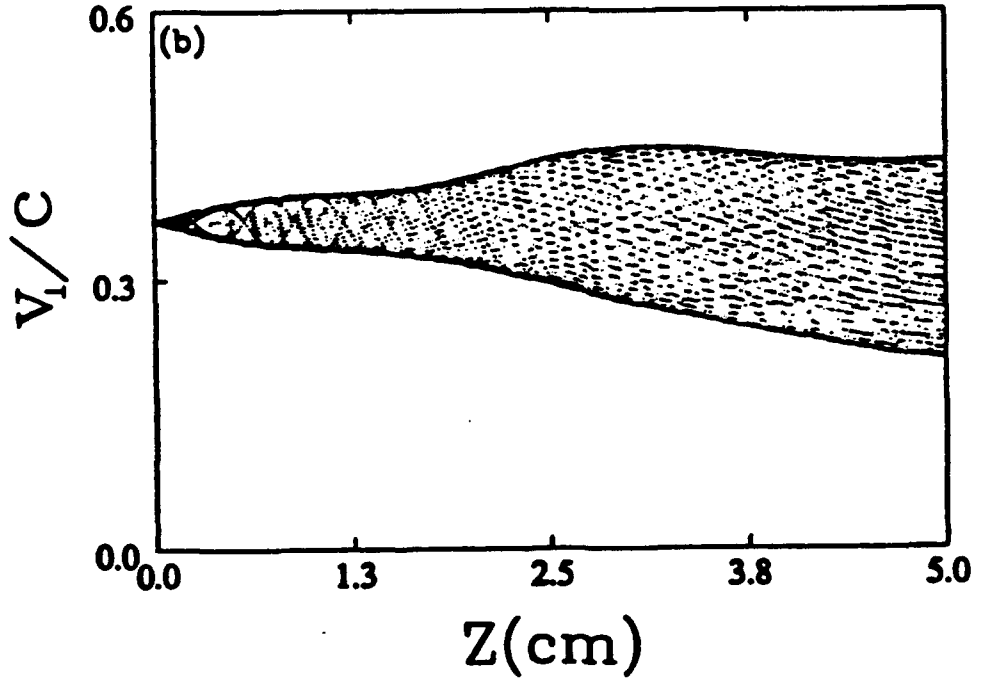
(b)
0.6
0.3
0.0
$V_\perp/C$
0.0
1.3
2.5
3.8
5.0
Z(cm)

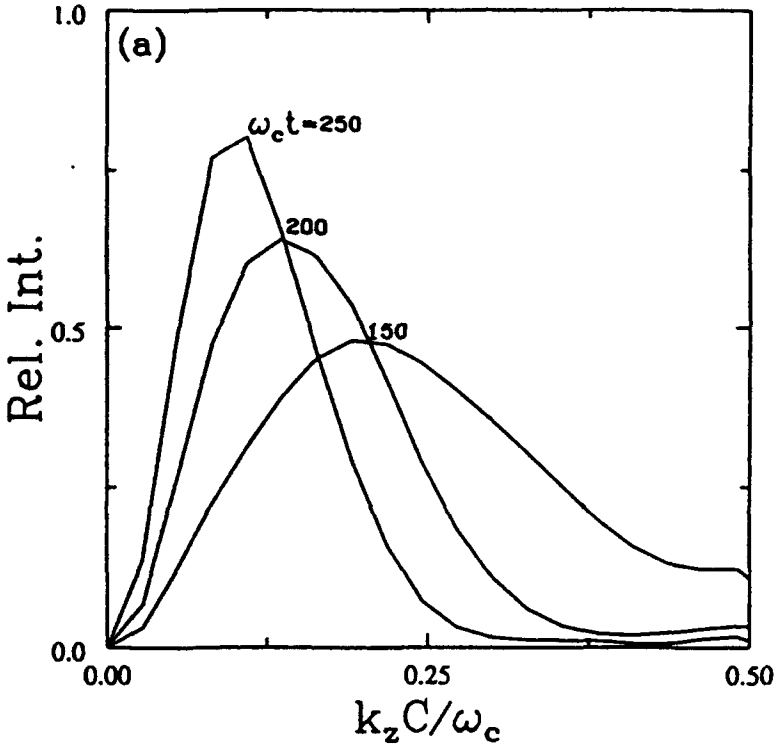
(a)
$\omega_c t$=250
200
150
Rel. Int.
1.0
0.5
0.0
0.00
0.25
0.50
$k_z C/\omega_c$

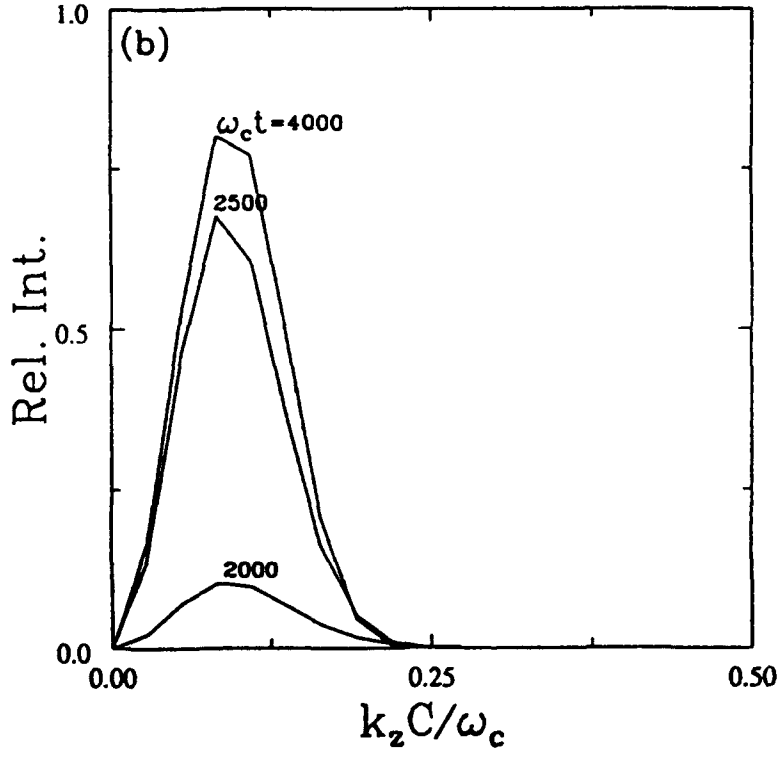
(b)
$\omega_c t$=4000
2500
2000
Rel. Int.
1.0
0.5
0.0
0.00
0.25
0.50
$k_z C/\omega_c$

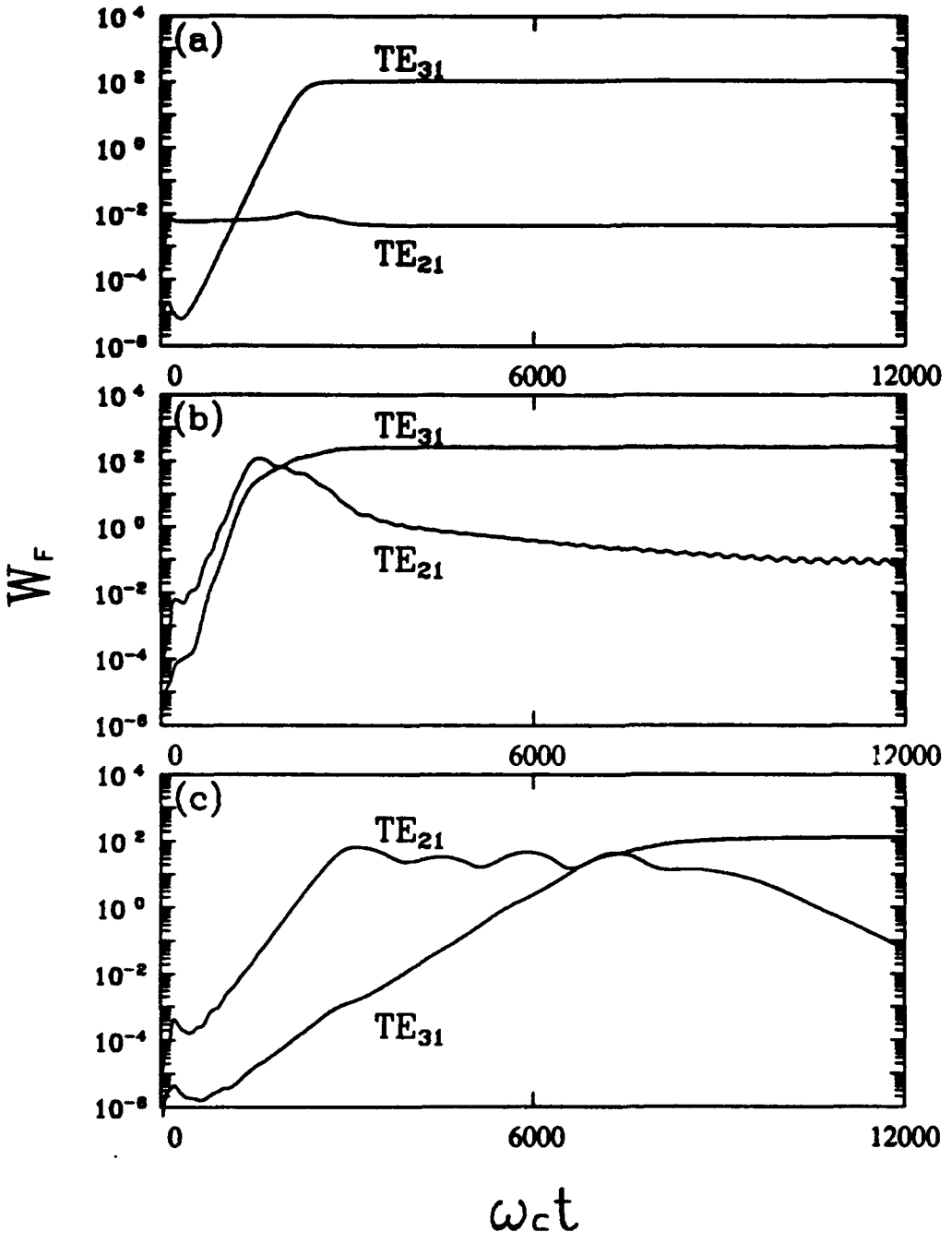
(a)
TE31
TE21
(b)
TE31
TE21
(c)
TE21
TE31
10⁴
10²
10⁰
10⁻²
10⁻⁴
10⁻⁶
0
6000
12000
W_F
ω_c t

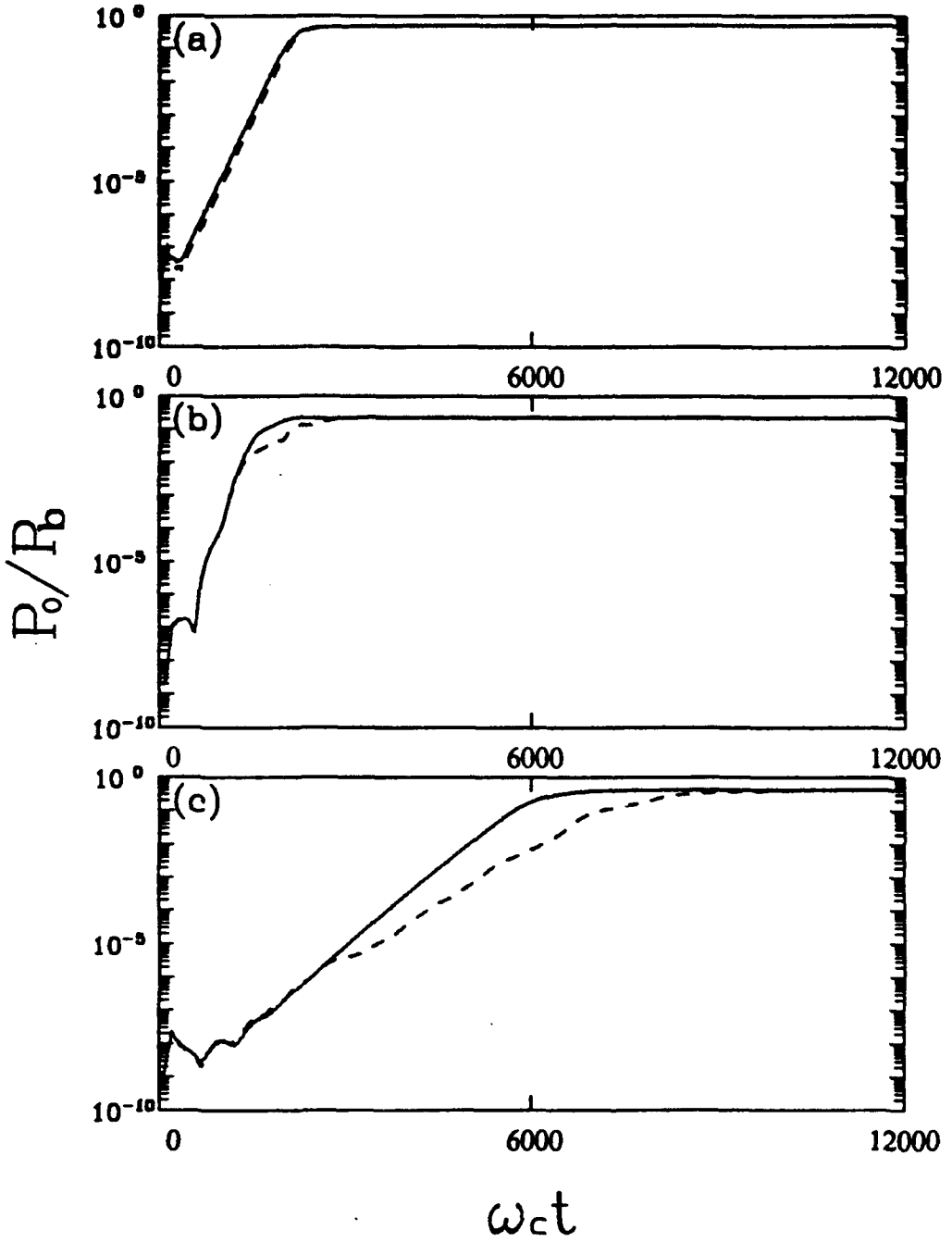
(a)
(b)
(c)
10^{0}
10^{-5}
10^{-10}
0
6000
12000
P_0/R_b
$\omega_c t$

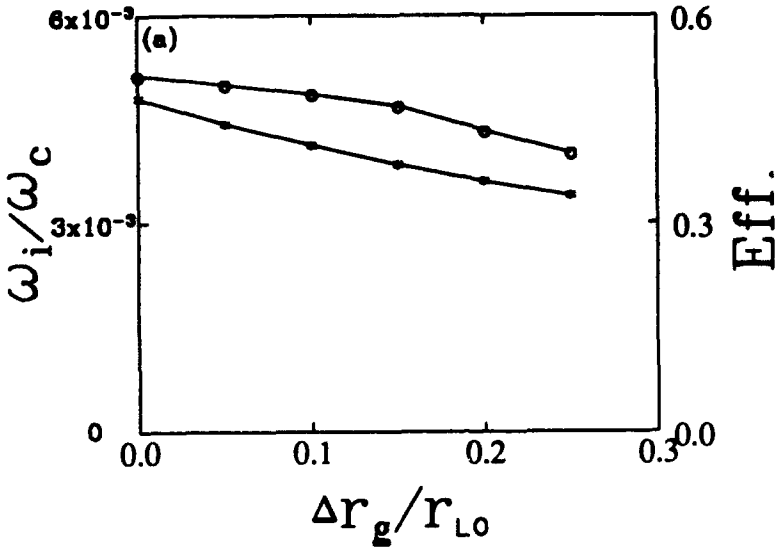
6x10⁻³
(a)
0.6
ω_i/ω_c
3x10⁻³
0.3
Eff.
0
0.0
0.0
0.1
0.2
0.3
Δr_g/r_LO

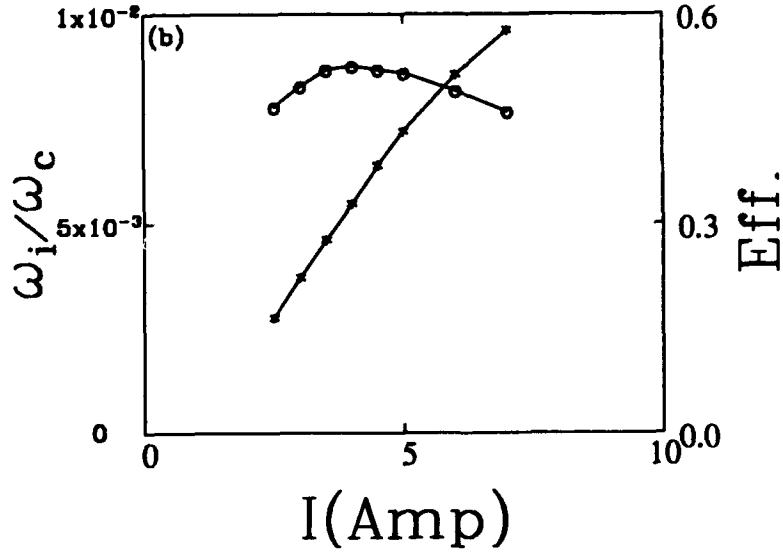
1x10⁻²
(b)
0.6
ω_i/ω_c
5x10⁻³
0.3
Eff.
0
0.0
0
5
10
I(Amp)

APPENDIX 2

Nuclear Instruments and Methods in Physics Research A 331 (1993) 541-544
North-Holland

NUCLEAR INSTRUMENTS & METHODS IN PHYSICS RESEARCH
Section A

A harmonic FEL based on the second harmonic gyroresonance

A.T. Lin
Department of Physics, University of California, Los Angeles, CA 90024, USA

K.R. Chu
Department of Physics, National Tsing Hua University, Hsinchu, Taiwan

The solenoidal guide field of Raman free electron lasers can be tuned to resonantly enhance a desired harmonic component of the electron quiver velocity. The feasibility of a harmonic FEL based on this effect is investigated. Computer simulations demonstrate that the gain and efficiency of the second harmonic generation can be comparable to that of the fundamental generation.

1. Introduction

In order to transport the high current beam (a few hundred A) through the wiggler region of a Raman FEL, an axially directed guide magnetic field is often employed to counter the defocusing effect of the space-charge field. The guide field exerts a strong influence on the electron equilibrium orbit [1-7] by which the gain, the operating frequency, and the output efficiency of a Raman FEL is affected. The importance of the guide field to the performance of an FEL was clearly demonstrated in a recent FEL amplifier experiment [8] in which the FEL efficiency was increased from 2% to 27% just by reversing the guide field direction. Recent multimode computer simulation results [9] suggest a possible interpretation of the dramatic contrast in efficiency: the normal field FEL provides more favorable conditions for superradiant amplification of local noise which degrades the beam quality and accounts for the much lower gain and efficiency.

The same experiment also revealed that in addition to the commonly observed dip in output power when the wiggler wavelength (λ_w) is close to the pitch ($\lambda_p = 2\pi v_z/\Omega_z$) of the electron gyration in the axial guide field, an unexpected dip occurs when $\lambda_w \approx -\lambda_p$. This was shown [7] to be the effect of harmonic gyroresonance of the off-axis electrons. Selective enhancement of a particular harmonic component of the electron quiver velocity by the guide field suggests the interesting possibility of harmonic FEL interactions. In this paper, a second harmonic FEL based on the harmonic gyroresonance effect is demonstrated through computer simulations.

2. Harmonic gyroresonance

Off-axis electron motion is not amenable to exact analysis. It has been studied numerically [3-5] or by some averaging method [5,6]. In these treatments, the harmonic aspect of the electron motion has been either obscured or averaged out. In ref. [7] we focused on the harmonic content of the electron motion by ignoring other first order complexities of the orbital motion, such as the betatron oscillation [5,6] and guiding center drift [3,5]. In that model [7], the magnetic forces of an off-axis electron is evaluated on an ideal helical orbit, as is projected in the cross-sectional plane in fig. 1a. The wiggler/guide field is expressed in the cylindrical coordinates (r, θ, z) by [2]

$$\boldsymbol{B} = B_0 \boldsymbol{e}_z + 2B_w \Big[I_1'(k_w r)\cos(\theta - k_w z)\boldsymbol{e}_r - \frac{I_1(k_w r)}{k_w r}\sin(\theta - k_w z)\boldsymbol{e}_\theta + I_1(k_w r)\sin(\theta - k_w z)\boldsymbol{e}_z \Big], \quad (1)$$

where $k_w = 2\pi/\lambda_w$, I_n is the modified Bessel function of the nth first kind, and I_n' is its derivative. In fig. 1a the electron phase angle is chosen so that in the limit $r_g \to 0$, the orbit reduces to the exact steady-state orbit.

Defining $\boldsymbol{e}_\rho$ and $\boldsymbol{e}_\phi$ as unit vectors perpendicular and tangential to the circle of fig. 1a, respectively, we may write the transverse component of the magnetic force as

$$\boldsymbol{F}_\perp = \frac{1}{c} eB_w \bar{v}_\parallel \{ [-I_0(k_w r) + I_2(k_w r)\cos 2\theta_1]\boldsymbol{e}_\rho + I_2(k_w r)\sin 2\theta_1 \boldsymbol{e}_\phi \}, \quad (2)$$

Table 1
Parameters and results of computer simulations

V	(beam energy)	700 keV
γ	(relativistic factor)	2.37
β	(v/c)	0.907
I	(beam current)	200 A
r_g	(initial beam radius)	0.128 cm
r_w	(waveguide radius)	0.255 cm
$\omega_c/2\pi$	(waveguide cutoff frequency)	34.5 GHz
λ_w	(wiggler period)	3.18 cm
B_0	(guide field)	14.2 kG
B_w	(wiggler field)	1 kG
f_0	(input frequency)	60 GHz
Γ	(gain)	1.2 dB/cm
η	(efficiency)	6%

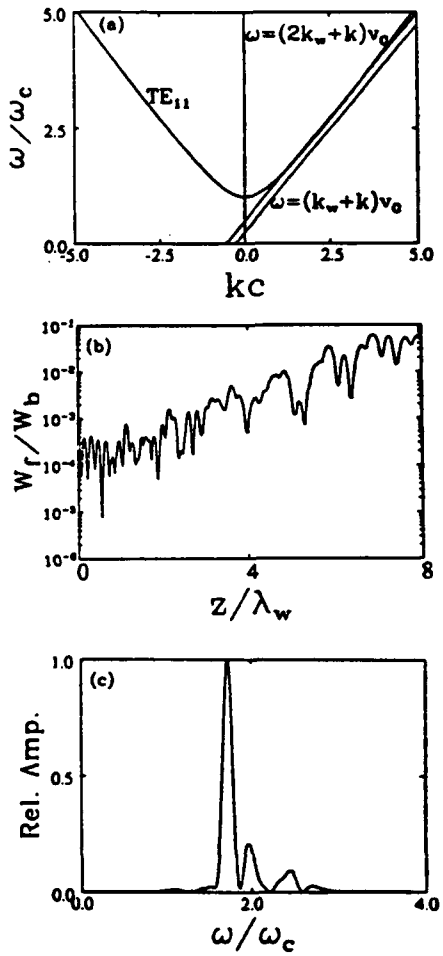

Fig. 2. Collective interaction. (a) Dispersion curves of the waveguide and beam modes, (b) the spatial growth profile of the injected signal, (c) the frequency spectrum at the output plane.

this configuration, only the second harmonic beam line is capable of interacting with the waveguide mode.

As is shown in eq. (9), the harmonic content of the electron quiver velocity is of the order of $(k_w r_g)^{|n-1|}$ for $k_w r_g < 1$. In order to confirm this scaling, the orbits of two electrons initially located at $r_g = 0.25 r_w$ and $0.5 r_w$ were followed in time with the magnetic field tuned at the second harmonic resonance. The y-component of the quiver velocity is displayed in ω-space in figs. 1b and 1c. The electron further away from the axis acquired a much stronger harmonic component while at the same time nearly grazed the waveguide wall. Therefore, we have chosen for our simulation an annular beam with $r_g = 0.5 r_w$. Using this beam, we carried out computer simulations of an FEL amplifier with a system length of eight wiggler wavelengths. The spatial growth of a 100 kW injected signal at $\omega_0 = 1.73\omega_c$ is shown in fig. 2b. The gain and efficiency estimated from simulation results are respectively 1.2 dB/cm and 6% which are comparable to that of the fundamental FEL amplifier. The spatial profile of the amplified signal also exhibits a regular beating structure. Spectral analysis carried out at the output plane (fig. 2c) reveals that in addition to the injected signal there are a few higher frequency modes (at substantial levels) with frequency separation of $\Delta\omega \approx n k_w v_0$ from the main mode. The interference of these modes with the injected signal results in the observed spatial field pattern and lower efficiency in comparision with the single mode simulation.

In conclusion, we have demonstrated the feasibility of a second harmonic FEL based on the gyroresonance effect with attractive gain and efficiency. Preliminary results also indicate a susceptibility to interference from higher harmonic modes.

Acknowledgements

This work was supported by the U.S. Air Force Office of Scientific Research under contract no. 91-0006 and The San Diego Supercomputing Center. We wish to thank Mrs. C.C. Lin for her numerical supports.

References

[1] L. Friedland, Phys. Fluids 23 (1980) 2376.
[2] P. Diament, Phys. Rev. A23 (1981) 2537..
[3] J.A. Pasour, F. Mako and C.W. Roberson, J. Appl. Phys. 53 (1982) 7174.
[4] R.H. Jackson, S.H. Gold, R.K. Parker, H.P. Freund, P.C. Efthimion, V.L. Granatstein, M. Herndon, A.K. Kinkead, J.E. Kosakowski and T.J. Kwan, IEEE J. Quantum Electron. QE-19 (1983) 346.

APPENDIX 3

Dependence of efficiency on magnetic field in gyro-backward wave oscillators

A. T. Lin and Chih-Chien Lin
Department of Physics, University of California at Los Angeles, Los Angeles, California 90024-1547

(Received 19 January 1993; accepted 17 March 1993)

A gyro-backward wave oscillator with its oscillation frequency close to the waveguide cutoff frequency has been experimentally demonstrated by other investigators to attain near 20% efficiency. Computer simulations have been carried out to elucidate the mechanisms which give rise to this high efficiency regime. The result shows that one of the plausible mechanisms is the resulting large frequency mismatch (detuning) which places the electron bunch in azimuthal phase close to where the maximum electron–wave coupling occurs.

I. INTRODUCTION

The gyrotron is a mature subject[1,2] and has been routinely built at various industrial companies for the use of electron cyclotron resonant heating in magnetic fusion devices. In order to achieve high efficiency, it often requires the magnetic field to satisfy grazing condition which limits its tunability. By raising the solenoidal magnetic field, the fundamental cyclotron line will eventually intersect the waveguide mode in the negative k_z direction of a ω (frequency) versus k_z (axial wave number) diagram (Fig. 1). In this region an electron beam carries its energy forward while the waveguide mode transports the generated wave energy backward. This provides an internal feedback mechanism and renders a cavity structure unnecessary. Furthermore, the relaxation of the grazing condition makes a gyro-backward wave oscillator (BWO) tunable by varying either the beam energy or magnetic field. Due to its tunability and simple configuration, gyro-BWO has recently been envisaged as a viable millimeter wave source.[3]

In the past there were a few theoretical analyses which determined the critical oscillation length of a gyro-BWO.[4,5] Lately, the theoretical approach had been improved to enable it to predict the eigenmode temporal growth rate of the oscillation.[6] An up-tapered magnetic field was observed[7] to increase the efficiency from around 10% to 30% and the mechanism responsible for the enhancement was recently identified.[8] Early experimental results[9] were able to obtain moderate efficiency but disappointing output power which was limited by the beam current. A recent experiment[10] employing high-energy electron beams was able to produce high-power (tens of megawatts) but low efficiency. Very recently, it was demonstrated[11] experimentally that operating close to the waveguide cutoff frequency, the efficiency of a gyro-BWO can reach around 20% with more than 100 kW output power. In this paper we shall, through computer simulations, offer a plausible explanation for the efficiency dependence on the solenoidal magnetic field in gyro-backward wave oscillators.

II. ELECTRON PHASE RELATIVE TO ELECTROMAGNETIC WAVE

The dominant bunching mechanism in electron cyclotron masers (gyro devices) is azimuthal phase bunching. The efficiency of the electron–wave interaction process depends on the phase of the bunched electrons relative to electromagnetic wave. To investigate how the change of magnetic field affects the device efficiency we shall start with a brief derivation of the equation governing the electron–wave energy exchange. Since a circularly polarized wave is a good approximation of the TE_{11} mode, which is the mode we are interested in, we assume that the electric field of the wave can be written as

$$\mathbf{E}=\frac{\omega}{c}|\mathbf{A}|(\hat{x}\cos\phi+\hat{y}\sin\phi), \tag{1}$$

where c is the speed of light, A is the vector potential, and $\phi=\omega t+k_z z$ is the phase of the backward propagating wave. The perpendicular velocity component of an electron moving in a uniform magnetic field can be expressed as

$$\mathbf{v}_\perp=v_\perp(\hat{x}\cos\psi+\hat{y}\sin\psi), \tag{2}$$

where ψ is the electron gyrophase angle. Define

$$\theta=\psi-\phi+(\pi/2) \tag{3}$$

as the electron phase relative to the wave. The addition of $\pi/2$ in the expression for θ is purely for the convenience of simulation diagnoses. The equation describing the time evolution of electron energy (γ) when it interacts with an electromagnetic wave is

$$\frac{d\gamma}{dt}=\frac{-e\mathbf{v}\cdot\mathbf{E}}{mc^2}=-a\omega\beta_\perp\sin\theta, \tag{4}$$

where m is the electron rest mass, $a=e|\mathbf{A}|/mc^2$, and $\beta_\perp=v_\perp/c$. Equation (4) clearly reveals that an electron loses energy when $\pi>\theta>0$ and gains energy when $2\pi>\theta>\pi$. The conversion of electron energy into wave energy is most efficient when $\theta=\pi/2$.

The resonant condition between a backward propagating electromagnetic wave (ω_0,k_0) and an electron in an axial magnetic field is

$$\Delta\omega=\omega_0+k_0v_z-(\Omega_e/\gamma)=0, \tag{5}$$

where Ω_e is the nonrelativistic electron cyclotron frequency. The electron phase versus distance is therefore roughly governed by the following equation:

 0899-8221/93/5(7)/2314/4/$6.00

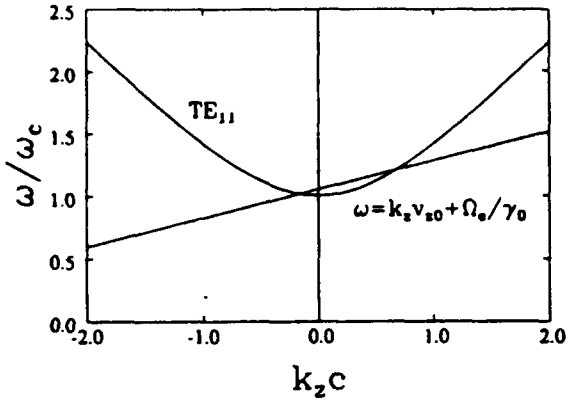

FIG. 1. The ω vs k_z diagram for a gyro-backward wave oscillator with $V=50$ kV, $\alpha=1.5$, and $\Omega_e/\gamma_0=1.05\omega_c$.

$$\theta=\theta_0+\left(\frac{\Omega_e}{\gamma}-\omega_0-k_0v_z\right)\frac{z}{v_{z0}}, \tag{6}$$

where θ_0 and v_{z0} are the electron phase and axial velocity at $z=0$. The phase shift can arise from the initial resonance mismatch (kinematic shift)

$$\theta_k=\left(\frac{\Omega_e}{\gamma_0}-\omega_0-k_0v_{z0}\right)\frac{z}{v_{z0}}, \tag{7}$$

where γ_0 is the electron relativistic factor at $z=0$ and the changes in γ and v_z result from the electron–wave interaction (dynamic shift)

$$\theta_d=-\left(\frac{\Omega_e}{\gamma_0^2}\Delta\gamma-k_0\Delta v_z\right)\frac{z}{v_{z0}}. \tag{8}$$

For the moment consider only the effect of the initial mismatch on the electron azimuthal phase bunching. An ensemble of electrons with initially equal transverse and axial velocities and randomly distributed in phase between 0 and 2π if perturbed by an electromagnetic wave which satisfies the exact resonance condition [Eq. (5)] will bunch at $\theta=\pi$. This is because the electron initially at $\theta=\pi$ will not be affected by the wave while the electrons in the neighborhood of π will either slow down (slip in phase) if their $\theta>\pi$ or speed up (gain in phase) if their $\theta<\pi$ by the wave. In this case the electrons on the average do not exchange energy with the wave. Now suppose that $\Delta\omega$ is positive. From Eq. (6) the electron phase trajectory will have a negative slope. This results in forming the electron bunch between 0 and π and the electrons on the average convert their kinetic energy into coherent radiation. The efficiency of the conversion process depends on where the bunch is located. The bunch location can be controlled by optimizing the initial mismatch (detuning) of an inject signal in an amplifier configuration.[12] It was also demonstrated that in a gyro-BWO configuration[9] the electron bunch can be placed at $\theta=\pi/2$ by properly up-tapering the magnetic field. In doing so, the efficiency was increased from around 10% for an untapered case to more than 30%. This was accomplished because the up-taper tends to increase the oscillation frequency and the amount of increase depends on the degree of tapering. On the other hand, in a uniform magnetic field situation (gyro-BWO) the initial mismatch may be changed by varying the magnetic field. This arises from the nonlinear relationship between ω and k_z when ω is close to the waveguide cutoff frequency. This is indeed true as will be verified in the next section through computer simulations.

TABLE I. Parameters used in computer simulations.

V	(beam energy)	50 kV
γ_0	(relativistic factor)	1.098
I	(beam current)	3 A
α	$(v_{\perp 0}/v_{z0})$	1.5
$\Delta v_{z0}/v_{z0}$	(velocity spread)	0.
ρ_b	(beam guiding center)	0.
r_w	(waveguide radius)	0.113 cm

III. EFFECTS OF VARYING MAGNETIC FIELD ON EFFICIENCY

One of the advantages of utilizing gyro-BWO as a millimeter wave source is its tunability through varying the magnetic field. Therefore it is important to investigate how the variation of magnetic field influences the output efficiency. In carrying out the simulations, only the TE_{11} waveguide mode was retained and the parameters used are shown in Table I and the magnetic field was varied so that the electron cyclotron frequency ranged from ω_c to $2\omega_c$ where ω_c is the waveguide cutoff frequency.

An uniform section of a waveguide with $L=3$ cm was employed and the output power came out from the beam entrance plane. Figure 2(a) shows the output efficiency and oscillation frequency versus the imposed magnetic field. As is expected the output frequency scales almost linearly with the magnetic field in the entire region covered in simulations except very near the cutoff. However, the output efficiency exhibits a significant jump (about 50%) when the oscillation frequency approaches the waveguide cutoff frequency. Simulation results clearly reveal that a roughly constant output power gyro-BWO can be operated in the following two regimes: high efficiency with about 8% tunability or medium efficiency with about 40% tunability. In the remaining part of this section, we shall elucidate the mechanism which causes the output efficiency to depend on the electron cyclotron frequency.

Two examples will be singled out to emphasize their difference. In the simulations the electromagnetic field is decomposed into two independent components (sine and cosine) in the azimuthal direction. Figure 3 displays only the results of sine component and the other component has similar behavior. The spatial distribution of electric field in steady state for $\Omega_e/\gamma_0=1.6\,\omega_c$ is shown in Fig. 3(a). From which the wave number of the dominant mode is estimated to be $k_0v_0=0.2135\omega_c$. The frequency spectrum of the electric field at $z=0$ is also shown in Fig. 3(a) and is peaked at $\omega_0=1.4\omega_c$. Substituting these results into Eq. (5) gives a frequency mismatch of $0.01\omega_c$. By reducing magnetic field to $\Omega_e/\gamma_0=1.05\omega_c$, the wave number and frequency of the dominant mode becomes $k_0v_0=0.053\omega_c$ and $\omega_0=1.043\omega_c$.

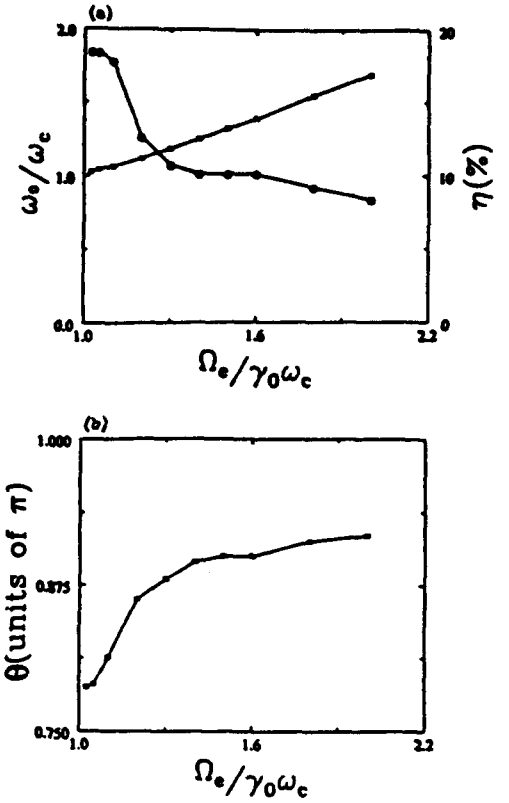

FIG. 2. Device performance versus magnetic field: (a) efficiency η (circles) and oscillation frequency ω_0 (stars) which show an increase of 50% in efficiency when ω_0 is close to ω_c and (b) bunch phase.

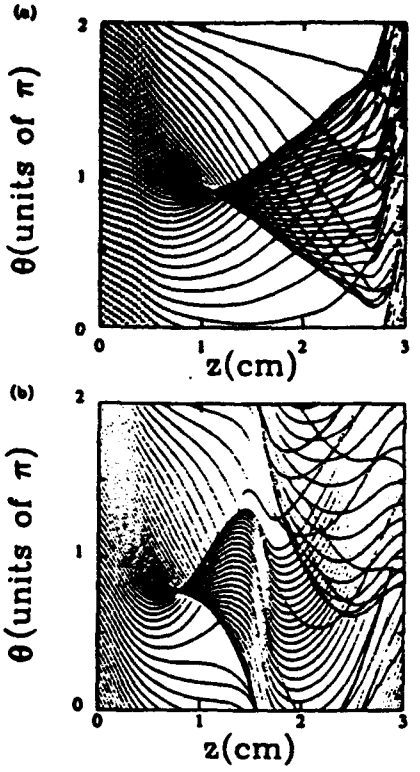

FIG. 4. Test electron azimuthal phase trajectories after $\omega_c t=2000$, (a) $\Omega_e/\gamma_0=1.6\omega_c$, (b) $\Omega_e/\gamma_0=1.05\omega_c$.

In this case the frequency mismatch is $0.046\omega_c$ which is more than four times the previous case. This is the consequence of nonlinear dependence of ω vs k_z (Fig. 1) when ω is close to ω_c. The effect of frequency mismatch on the output efficiency will become clear after examining Fig. 4.

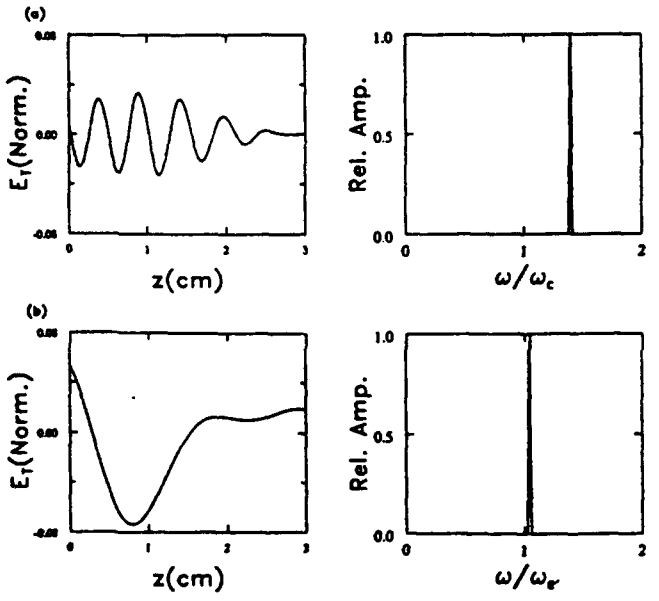

FIG. 3. Electric field spatial distribution and the output frequency spectrum after the system reaches steady state: (a) $\Omega_e/\gamma_0=1.6\omega_c$ and (b) $\Omega_e/\gamma_0=1.05\omega_c$.

In order to illustrate how the electron azimuthal bunching process differs when the magnetic field is varied, the phase trajectories of 40 test electrons initially ($z=0$) uniformly distributed between 0 and 2π are followed. In simulations, the electron phases are evaluated at the instantaneous position of the electron and after the system has reached steady state. The results of using $\Omega_e/\gamma_0=1.6\omega_c$ are given in Fig. 4(a). According to Eq. (6) the initial slope of the phase trajectory is negative if the frequency mismatch ($\Delta\omega$) is positive. In the region of $\pi<\theta<2\pi$, the electron–wave interaction results in a positive $\Delta\gamma$ and therefore the phase trajectory becomes more negative while in the region of $0<\theta<\pi$ the negative slope should be reduced. These detailed phase shift phenomena are all clearly demonstrated in simulation results [Fig. 4(a)]. In this case the electrons eventually bunch at $\theta\simeq\frac{7}{8}\pi$ and $z\simeq 1$ cm. As a result of the larger initial frequency mismatch for $\Omega_e/\gamma_0=1.05\omega_c$, the electrons bunch [Fig. 4(b)] around $\theta\simeq\frac{3}{4}\pi$ which is substantially closer to $\theta=\pi/2$ (maximum electron–wave coupling) than the previous case. The variation of the bunch phase versus magnetic field is shown in Fig. 2(b). The resulting phase behavior follows the efficiency curve quite closely. This further supports the assertion that the final bunch phase plays a decisive role in determining the output efficiency of a gyro-BWO. At the same time the group velocity of the wave in the latter case is also slower which increases the electron–wave interaction time. These have all contributed to the enhancement of output efficiency of the latter case. An attempt has also been made to study the effects of tapering the magnetic

field when ω_0 is close to ω_c. Preliminary results show that the output power starts to oscillate even with a relatively small up-tapering. A more detailed investigation is needed.

IV. SUMMARY

Computer simulations have been performed to demonstrate that a gyro-backward wave oscillator operated at ω_0 close to the waveguide cutoff frequency produces far more output power. It was illustrated that one of the plausible mechanisms for this high efficiency operation is the resulting substantially larger frequency mismatch (detuning) which places the electron bunch close to $\theta=\pi/2$ where the maximum electron–wave coupling takes place. To increase the efficiency further, by up-tapering the magnetic field, more studies are needed.

ACKNOWLEDGMENTS

This work was supported by the Air Force Office of Scientific Research under Grant No. AFOSR 91-0006 and the San Diego Supercomputing Center.

[1] V. A. Flyagin, A. V. Gaponov, M. I. Petelin, and V. K. Yulpatov, IEEE Trans. Microwave Theory Tech. MTT-25, 514 (1977).
[2] J. L. Hirshfield and V. L. Granatstein, IEEE Trans. Microwave Theory Tech. MTT-25, 522 (1977).
[3] M. Caplan, *Conference Digest of the 12th International Conference on Infrared and Millimeter Waves*, Orlando, Florida, 1987 (Institute of Electrical and Electronic Engineers, New York, 1987), p. 276.
[4] J. M. Wachtel and E. J. Wachtel, Appl. Phys. Lett. 37, 1059 (1980).
[5] S. Y. Park, R. H. Kyser, C. M. Armstrong, R. K. Park, and V. L. Granatstein, IEEE Trans. Plasma Sci. PS-18, 321 (1990).
[6] A. T. Lin and P. K. Kaw, Int. J. Electron. 72, 887 (1992).
[7] A. K. Ganguly and S. Ahn, Appl. Phys. Lett. 54, 514 (1989).
[8] A. T. Lin, Phys. Rev. A 46, R4516 (1992).
[9] S. Y. Park, R. H. Kyser, C. M. Armstrong, R. K. Park, and V. L. Granatstein, IEEE Trans. Plasma Sci. PS-16, 90 (1990).
[10] T. A. Spencer, R. M. Gilgenbach, and J. J. Choi, J. Appl. Phys. 72, 1221 (1992).
[11] C. S. Kou, S. H. Chen, L. R. Barnett, and K. R. Chu, Phys. Rev. Lett. 70, 924 (1993).
[12] T. H. Kho and A. T. Lin, Phys. Rev. A 40, 2486 (1989).